Proceedings of the 4th WSEAS International Conference on Fluid Mechanics and Aerodynamics, Elounda, Greece, August 21-23, 2006 (pp370-375)

Application of Swirl Generators to Enhance Performance of Waterheads on Liquid Coolers

SHYAN-FU CHOU & CHIA-CHIEN CHU
Department of Mechanical Engineering
National Taiwan University
No.1, Roosevelt Rd. Sec 4, Taipei, Taiwan
Republic of China

Abstract: - In this study, both numerical and experimental studies have been made to investigate the influence of swirl generators on waterheads in the application of heat-removing devices such as liquid coolers in PC industries. The main objective of this research is to improve the heat transfer efficiency of waterheads. Traditional way of enhancing the efficiency is by increasing the effective fin area inside. The unavoidable way of doing so is to stuff more fins into the given geometry and therefore the pressure drop across the waterhead substantially increases. Our innovative strategy is to confine the fluid flow path and use a mechanism to generate swirl flow around the pin fins which have a far less number than typical fins. With laboratory experiments and numerical modeling, it is shown that the waterhead performance indeed improves with the addition of swirl generators. By employing the appropriate type of generators, it is possible to achieve 15-20% decrease in overall thermal resistance. For a Reynolds number of $1*10^5$-$2*10^5$, the pressure drop is also kept at reasonable amount. Overall, our results show that it is possible to optimize the design of waterheads to achieve the desired heat transfer and pressure drop goals.

Key-Words: - Swirl generator, waterhead, liquid cooler

1 Introduction

In air-cooled applications, the air flow generated by the fan is responsible for quickly transferring the heat conducted by the heat sinks from the surface of the package to the ambient. The larger the amount of the heat needed to be removed, the higher the fan RPM and also the denser the fins. When the fan RPM is too high to remain at acceptable noise level or when the fin number reaches its limit, the demand for liquid cooling arises. Liquid cooling system consists of following essential components: waterhead, pump, radiator and tank. Liquid, for example water, is forced to go through several rows of fins in the waterhead by pumps. The waterhead designer has traditionally been forced to rely heavily on the increasing of fin number and thus the heat transfer area, while the pressure drop across the waterhead significantly increases. The manufacturing of these parts is also getting more and more difficult as the gap between fins miniaturizes to the extent that the wear of tools becomes a considerable cost.

Therefore, the objectives of our study are as following:

(1) Improve the overall heat transfer coefficient of waterheads in liquid cooling system as compared with current practice of using machined fins.
(2) Minimize the pressure drop increase across the waterhead as a result of employing the proposed heat transfer enhancement techniques on the bottom of fins.
(3) Reduce the cost of tool wear by increasing the distance between fins.

Several studies have been made on the formation of swirl flow and vortex. Hagiwara et al. [1] established a model of vortex breakdown flow in a quarl burner and the results showed that the flow in the swirl flow generating pipe is close to solid-body rotation. A complex two-celled, near-axis inner recirculation zone (IRZ) takes shape in further downstream and this is thought to be a manifestation of bubble-type vortex breakdown. The vortices increase the amount of heat transfer as the temperature gradient near the wall increases. Swirl can lead to three-dimensional flow, where circumferential velocity can become as large as the axial velocity. The vortices will increase wall shear, which leads to increased pressure drop.

Lilley and Rhode [2] developed a numerical code named STARPIC (Swirling Turbulent Axisymmetric Recirculation Practical Isothermal Combustor) to calculate the axisymmetric swirl turbulent isothermal flow field. The results show that numerical results based on very simple physical model can be in good agreement with the experimental data. The presence of a large central recirculation zone indeed efficiently increases the amount of heat transfer.

Swirl flow affects heat transfer with the change of the state of developing boundary layers, votices and flow destabilization. The heat transfer enhancements are mainly located in the downstream region of the vortex. Therefore, if the swirl generators are placed in the right location to let the wake region in the meanwhile also the region with most heat generated. Since the swirl flow is three-dimensional, convective heat transfer is enhanced according to both longitudinal and radial velocities.

Therefore, we construct a series of experiments in the hope of demonstrating the benefits of applying swirl generators on the fins to improve the heat transfer efficiency. In the mean time, we have also performed several cases of simulations to demonstrate the applicability of simulation software on the analysis of test conditions. Two commercially available computational fluid dynamics code, FLUENT and FLOTHERM are used to model both fluid flow and heat transfer in various configurations with and without swirl generators.

2 Problem Formulation

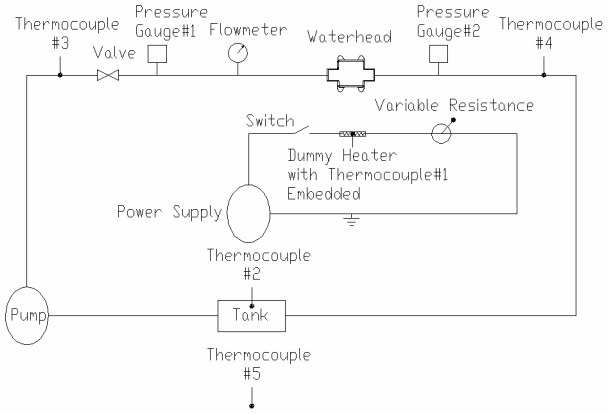

Fig. 1 Schematic of experiment system

Schematic of experiment is shown in Fig. 1, the pump inputs water from the tank to the circuit. With the combination of valves and flowmeters, we can precisely control the flow rate in the whole system. Pressure gauges are also used before and after the waterhead to monitor the pressure drop. The diameter of all pipes and barbs is 3/8". The bottom contact area of waterhead is 32.5*32.5 mm, which is a popular value for commercial CPUs. The height of waterhead is specified to be 20 mm, and the inside dimension is 29*29 mm. To investigate the differences between traditional fin type waterhead and the one with swirl generators, we made 5 models with different design concepts and geometries as described below.

2.1 Test Specimen and Experiment Condition

All 5 models of test specimen are shown in Fig. 2. Model 1 and 2 are the traditional fin type heat sinks and their only difference is that Model 1 has 7 2-mm-thick fins while Model 2 increases to 13 1mm-thick fins. Model 3 is a comparison to Model 4 and 5 which have swirl generators on the roots of the fins. For model 3, totally 49 pieces of 2mm-diameter pin fins are arranged in pattern while a block with corresponding 3mm-diameter holes are assembled to confine the fluid in the flow paths. As for model 4 and 5, the number of pin fins is further reduced to 25 while the diameter of pin fins remains the same. To accommodate the swirl generators, the diameter of the holes on the matching blocks is increased to 4mm. All the blocks mentioned above have some specially cut inlet and outlet domain to facilitate the flow into the block, through all cylinder surfaces and out to the exit.

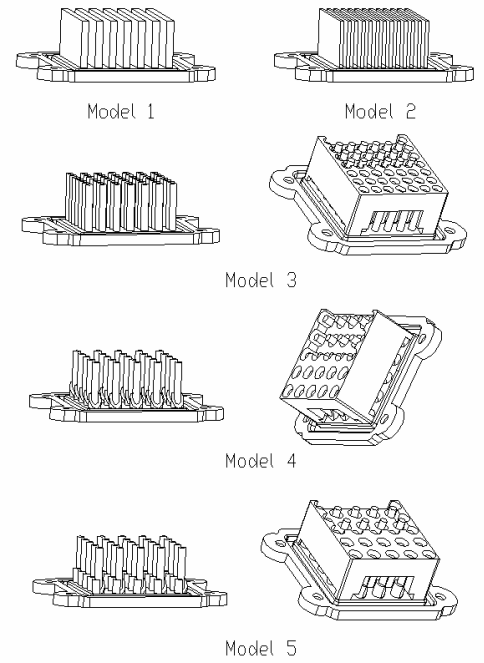

Fig. 2 The geometry of test specimen

For Model 1-5, we use two kinds of frequently encountered materials in cooler industry to do the test specimen. One is aluminum AL6051 and the other is copper C1100. Thus we can investigate the influence of copper's high thermal conductivity on the overall efficiency of waterheads.

2.2 Analytical analysis

As described above, analytically we can obtain an exact solution of the heat conducted from the bottom of fins and finally dissipated to the ambient by convection. Assuming a one-dimensional fin exposed to the ambient where the temperature is T_∞.

If the base temperature of the fins is T_0, the heat conduction and convection on a small volume with thickness dx gives:

(1) Heat conducted from the base side:

$$q_x = -kA\frac{dT}{dx}$$

(2) Heat conducted to the fin tip side:

$$q_{x+dx} = -kA\frac{dT}{dx}|_{x=dx} = -kA\left[\frac{dT}{dx} + \frac{d^2T}{dx^2}dx\right]$$

(3) Heat loss to the ambient by convection:

$$q_{conv} = hPdx(T - T_\infty)$$

Where A is the cross sectional area of the fin, P is the perimeter.

The energy equilibrium on this small volume gives

$$\frac{d^2T}{dx^2} - hP(T - T_\infty) = 0 \quad (1)$$

Let $\theta = T - T_\infty$, eqn. (1) becomes

$$\frac{d^2\theta}{dx^2} - \frac{hP}{kA}\theta = 0 \quad (2)$$

When the length of the fin is finite and convection also occurs on the fin tip, one of the boundary conditions is:

$$\theta = \theta_0 = T_0 - T_\infty \text{ at x=0} \quad (3)$$

Applying this BC into eqn. (2) and we can get the result after some algebraic calculations.

$$\frac{T - T_\infty}{T_0 - T_\infty} = \frac{\cosh m(L-x) + (\frac{h}{mk})\sinh m(L-x)}{\cosh mL + (\frac{h}{mk})\sinh mL} \quad (4)$$

The total heat transferred can be calculated by integrating the convective heat loss:

$$q = \int_0^L hP(T - T_\infty)dx = \int_0^L hP\theta dx \quad (5)$$

Finally, the analytical solution of the total heat transfer on a 1D fin is

$$q = \sqrt{hPkA}(T_0 - T_\infty)\frac{\sinh mL + (\frac{h}{mk})\cosh mL}{\cosh mL + (\frac{h}{mk})\sinh mL} \quad (6)$$

When the x direction is the only source of temperature gradient, we can use eqn. (6) to estimate the total heat transfer on a single fin.

2.3 Numerical analysis

2.3.1 Turbulence Modeling

In this study we choose the standard two-equation $k-\varepsilon$ model with RNG modifications as the turbulence model. The isotropic eddy viscosity is calculated using values of turbulence energy k and dissipation rate ε obtained from their respective transport equations in this approach. However, the isotropic assumption for the eddy viscosity also becomes the major limitation for its application. Therefore, different stress models are used to improve computational accuracy and the examples are the Algebraic Stress Model (ASM) [3] and the Reynolds Stress Model (RSM) [4]. According to Sloan et al. [5], the ASM model has better predictions for the flow field variables in most cases while the performance is no better than the $k-\varepsilon$ model for a confined, swirling flow field. As for the RSM model, it requires relatively large amount of CPU time and memory and also sometimes rather difficult to reach a convergent solution. Therefore, we choose the commonly used values for the empirical constants in this model as:

$$C_\mu = 0.09, \sigma_k = 1.0, \sigma_\varepsilon = 1.3$$

$$C_{1\varepsilon} = 1.44, C_{2\varepsilon} = 1.92$$

The inlet values of k and ε are prescribed in accordance with the following equations:

$$k_{in} = 0.03 * u_{in,}^2 \varepsilon = \frac{k_{in}^{1.5}}{0.025\overline{D}_0} \quad (7)$$

Where $\overline{D}_0$ is the inlet diameter.

2.3.2 Flow Model and Numerical Method

In conservative form, the three-dimensional continuity and momentum equations describing the inviscid incompressible flow are as following:

$$\frac{\partial\vec{U}}{\partial t} + \frac{\partial\vec{F}}{\partial x} + \frac{\partial\vec{G}}{\partial y} + \frac{\partial\vec{H}}{\partial z} = 0 \quad (8)$$

The vector $\vec{U}$, which contains unknown variables can be written as:

$$\vec{U} = \begin{bmatrix} p/\rho_0 \\ u \\ v \\ w \end{bmatrix}$$

While the rest flux vectors $\vec{F}$, $\vec{G}$ and $\vec{H}$ are:

$$\vec{F} = \begin{bmatrix} c^2u \\ u^2 + p/\rho_0 \\ uv \\ uw \end{bmatrix}, \vec{G} = \begin{bmatrix} c^2v \\ uv \\ v^2 + p/\rho_0 \\ vw \end{bmatrix},$$

$$\vec{H} = \begin{bmatrix} c^2 w \\ uw \\ vw \\ w^2 + p/\rho_0 \end{bmatrix}$$

Where c is the pseudospeed of sound and is described in the pseudocompressibility approach [6].

All the flow properties are nondimensionalized by using the inlet pressure ($\overline{P}_0$), density ($\overline{\rho}_0$) and inlet diameter ($\overline{D}_0$) in the following way:

$$L = \frac{\overline{L}}{\overline{D}_0}, p = \frac{\overline{p}}{\overline{P}_0}, t = \frac{\overline{t}}{\overline{D}_0}\sqrt{\frac{\overline{P}_0}{\overline{\rho}_0}}$$

$$u, v, w = \frac{\overline{u}, \overline{v}, \overline{w}}{\sqrt{\overline{P}_0/\overline{\rho}_0}} \quad (9)$$

The governing equations are solved explicitly by means of the finite volume technique and the time-marching approach. The time discretization is done by using the modified four-step Runge-Kutta scheme.

3 Results and Discussion

3.1 Simulation Results

The experimental conditions are modeled by using the commercial CFD software FLUENT and FLOTHERM. The FLUENT code uses a control volume technique to convert the governing equations to algebraic equations that can be solved numerically. Discrete equations are obtained after integrating the governing equations about each control volume. FLUENT stores discrete values of the conserved quantity at the cell centers and determines the face values of the conserved quantity for the convective terms by an upwind technique. Here the pressure-velocity coupling was resolved using the SIMPLEX procedure.

With the assistance of FLOTHERM in which we use automatic algebraic method as turbulence modeling technique, we find that results in FLOTHERM agree well with that in FLUENT. Since both the time needed for the construction of models and the required CPU time are less in FLOTHERM when the grid numbers are approximately the same, it is preferred when time efficiency is a major concern. The working fluid is water, and inlet conditions are uniform 25℃ at 1 atm. The flow rates are specified to be 15 g/sec and 20 g/sec, therefore the corresponding Reynolds numbers are $1.04*10^5$ and $1.39*10^5$.

For Model 1, since the distance between fins is 2 mm, it does not exert much resistance on the flow. It can also be observed that when Power=80 W and the heat sink material is aluminum, the corresponding temperature field has a temperature difference between fin base and tip as large as 10 ℃. When the heat sink material is changed from aluminum to copper, we can immediately find the base-tip temperature difference reduced to within 6 ℃. The effect of changing material also reduces the resulting case temperature (T_{case}) as high as 2.5 ℃ when the power is 100 W.

Similar results can be obtained from Model 2, the temperature difference between fin base and tip for aluminum heat sink is also over 10 ℃. The effect of changing heat sink material from aluminum to copper results in a 2.4 ℃ decrease of case temperature.

For Model 3 which is simply cylindrical pin fins with flow confinement blocks, the simulation results show that it can decrease T_{case} by 2.1 ℃ when the power is 100 W. The use of copper heat sink further reduces T_{case} by approximately 2.3 ℃ and the temperature difference between fin base and tip can also be as small as 5 ℃.

With the addition of swirl generators on the bottom of fins, the simulation results indeed demonstrate the swirl motion as shown in Fig. 3, which is the velocity filed in y cross section.

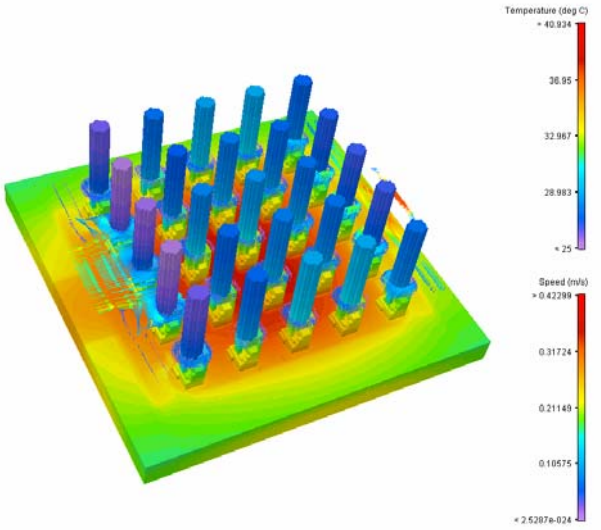

Fig. 3 Fin surface temperature distribution with velocity filed at y=0.5H for Model 4 ($Re=1.04*10^5$, Power=90 W)

The effect of more rapid heat removing can also be observed from Fig. 3, in which the original high temperature area of the 32.5*32.5 mm heat source shrinks to be less than 29*29 mm. When the material of heat sink is replaced with copper, the same

phenomenon can still be observed. The net decrease in T_{case} compared with aluminum heat sink is 1.7℃. The velocity field for Model 5 is shown in Fig. 4, which displays a more uniform distribution of the flow velocity. However, the resulting T_{case} is not that satisfying compared to Model 4 as shown in Fig. 5. In fact the T_{case} for Model 5 may be higher than that of Model 4 by 2.3℃ when the power is 100 W. After further investigation into the resulting pressure distribution, we found that the pressure loss of Model 5 is 250 Pa, which is about 25% higher than that of Model4. The root cause is the high flow resistance induced by the vertical walls of the swirl generators. These vertical walls in one way force the fluid to flow directly to the slope of swirl generators and one the other way block half of the original flow passage. Therefore, the net flow rate is actually much less than Model 4 and of course the heat-removing efficiency also reduced.

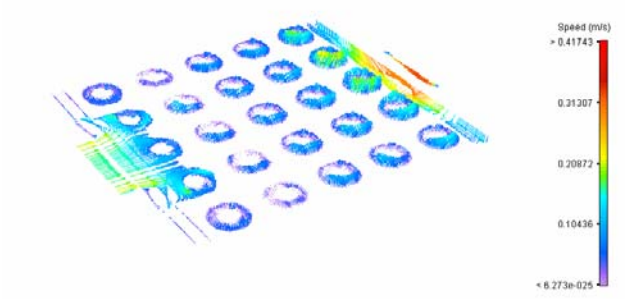

Fig. 4 Velocity field at y=0.5H for Model 5 (Re=1.39*10^5, Power=70 W)

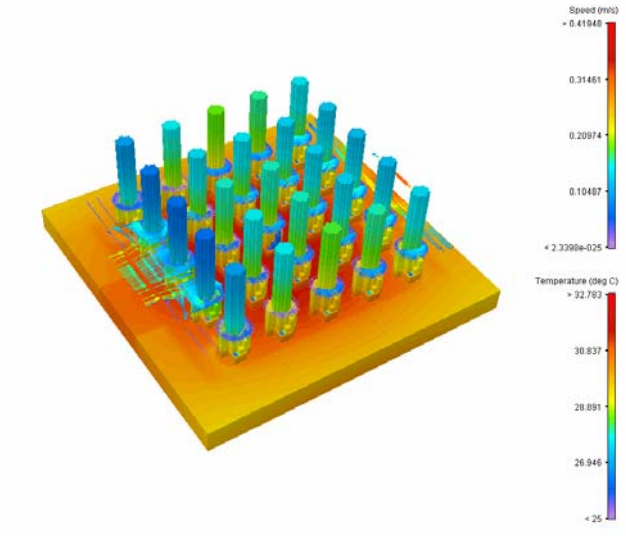

Fig. 5 Fin surface temperature distribution with velocity filed at y=0.5H for Model 5 (Re=1.39*10^5, Power=50 W)

In summary, the correlations between the power dissipated and T_{case} for all the models described are shown in Fig. 6 when Re=1.04*10^5. Similar trend can be found with the case of Re=1.39*10^5 except that T_{case} is lower compared with its corresponding cases. The correlation curves show good agreement with the definition of thermal resistance, which specifies that (T_{case}-T_{amb}) should be proportional to power dissipated under the same geometry and construction.

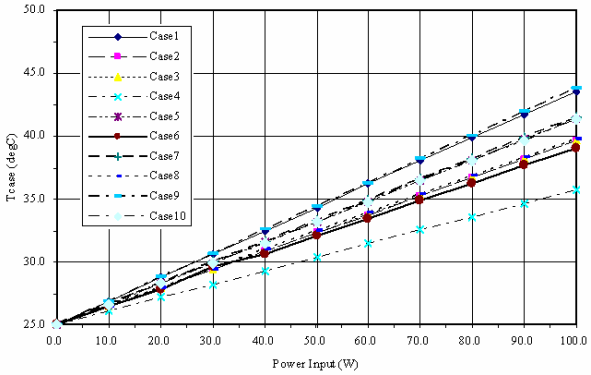

Fig. 6 Simulation results of case temperature T_{case} as a function of power dissipated for 5 models with different materials (Re=1.04*10^5)

3.2 Experimental Results

Results of actual tests are shown in Fig. 7. These test results also show the trend that (T_{case}-T_{amb}) is proportional to power dissipated under the same geometry and construction. By dividing the actual test result T_{case}, we can obtain the deviation of simulation from actual test results in percentage as shown in Fig. 8 and 9. For Re=1.04*10^5, the deviation is ranging from -5% to 15%. For several cases, the maximum of deviation occurs at power=30W. Based on the specified condition that the ambient temperature is controlled at 25℃, the deviation at 0 W is definitely 0% at the original in Fig. 7. While as the power increases, the temperature rise remains small at first and later gradually increases. Therefore the simulation error will be scaled up as the denominator is still relatively small in the vicinity of 30W.

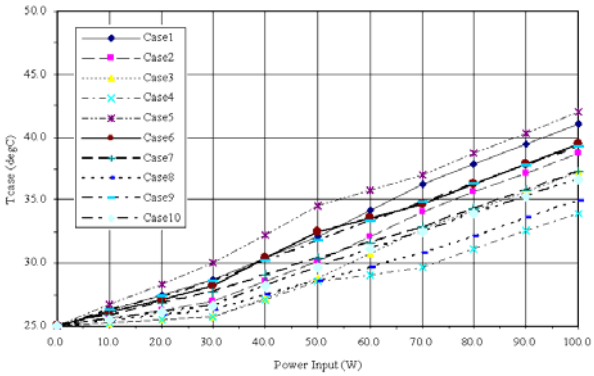

Fig. 7 Measured results of case temperature T_{case} as a function of power dissipated for 5 models with different materials (Re=1.04*10^5)

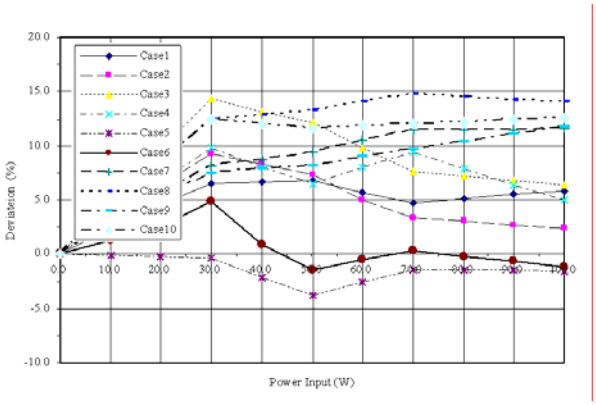

Fig. 8 Deviation of simulation vs. actual test results as a function of power dissipated for 5 models with different materials ($Re=1.04*10^5$)

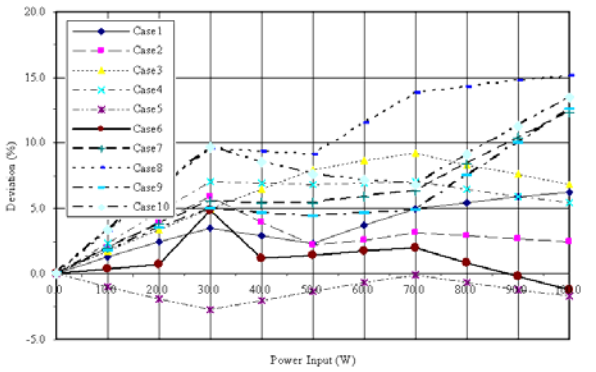

Fig. 9 Deviation of simulation vs. actual test results as a function of power dissipated for 5 models with different materials ($Re=1.39*10^5$)

For $Re=1.39*10^5$, the deviation is ranging from -2.5% to 15%. The phenomenon of maximum deviation occurring at power=30W still exists while for some cases the deviation increases with the power. However, all of the deviations are kept under 15% which is an acceptable range when we take into consideration the experimental error and simulation simplification.

As for the concern of pressure drop before and after the waterhead, the pressure gauge readings show that the largest drop is 247.9 Pa for Model 5 while the second largest is 205.6 Pa for Model 4. As discussed in the previous section, the design of Model 5 has a vertical wall for each pin fin and forms a rather large resistance when the fluid passes it. The pressure drop for Model 3 is 210.1 Pa which is approximately the same as Model 4. This is because the gap between each pin fin and the surrounding confining block is merely 0.5mm. In comparison, the respective pressure drop values for Model 1 and 2 are 65.8 Pa and 95.1 Pa.

4 Conclusion

The calculated and measured variations in the thermal performance of the waterheads are in good agreement. Taking the assumptions made in the geometrical modeling of the swirl generators into consideration, some minor differences between the calculated and measure results are acceptable. The advantages of swirl generators have been clearly identified as the maximum T_{case} decrease by using swirl generators can be as large as 7 ℃. The results also indicate that the pressure drop increase can be kept at an acceptable level. Calculated and measured results of the waterheads suggest that:

(1) The advantage of swirl flow over non-swirling flow is identified in the application of heat dissipation. Both calculated and measured results successfully predict the trend of temperature decreasing.

(2) Further investigation can be applied on the geometrical design of pin fins and the corresponding confining block to lower the level of pressure drop increase while maintaining the merit in excellent heat removing.

(3) The effect of Reynolds number on the thermal performance has not been fully investigated. In the near future, we will conduct further studies on a large range of Reynolds number to analyze the effect and optimize the design of swirl generators according to the exact application conditions.

References:

[1] A. Hagiwara, S. Borz and R. Weber, Theoretical and experimental studies on isothermal expanding swirling flows with application to swirl burner design-results of the NFA 2-1 investigations, *International Flame Research Foundation*, Technical Report Doc. F 259/a/3, 1986

[2] D. G. Lilley and D. L. Rhode, A computer code for swirling turbulent axisymmetric recirculating flows in practical isothermal combustor geometries, *NASA Contractor Report 3442*, 1982

[3] W. Rodi, Examples of turbulence models for incompressible flows, *AIAA J.*, Vol. 20, 1982, pp. 872-879.

[4] K. Hanjalic, B.E. Launder and E. Schiestel, Multiple time-scale concepts in turbulent transport modeling, *Turbulent Shear Flow*, Vol. 2, 1979

[5] D.G. Sloan, P.J. Smith and L.D. Smoot, Modeling of swirl in turbulent flow systems, *Prog. In Energy and Combustion Science*, Vol. 12, 1986, pp. 163-250

[6] A.J. Chorin, A numerical method for solving incompressible viscous flow problems, *Journal of Computational Physics*, Vol. 2, 1967, pp. 12-26